Delft University of Technology

Lightly strained germanium quantum wells with hole mobility exceeding one million

Lodari, M.; Kong, O.; Rendell, M.; Tosato, A.; Sammak, A.; Veldhorst, M.; Hamilton, A. R.; Scappucci, G.

DOI
10.1063/5.0083161

Publication date
2022

Document Version
Final published version

Published in
Applied Physics Letters

Citation (APA)
Lodari, M., Kong, O., Rendell, M., Tosato, A., Sammak, A., Veldhorst, M., Hamilton, A. R., & Scappucci, G. (2022). Lightly strained germanium quantum wells with hole mobility exceeding one million. *Applied Physics Letters*, *120*(12), Article 122104. https://doi.org/10.1063/5.0083161

Important note
To cite this publication, please use the final published version (if applicable).
Please check the document version above.

Copyright
Other than for strictly personal use, it is not permitted to download, forward or distribute the text or part of it, without the consent of the author(s) and/or copyright holder(s), unless the work is under an open content license such as Creative Commons.

Takedown policy
Please contact us and provide details if you believe this document breaches copyrights.
We will remove access to the work immediately and investigate your claim.

This work is downloaded from Delft University of Technology.
For technical reasons the number of authors shown on this cover page is limited to a maximum of 10.

Green Open Access added to TU Delft Institutional Repository

'You share, we take care!' - Taverne project

https://www.openaccess.nl/en/you-share-we-take-care

Otherwise as indicated in the copyright section: the publisher is the copyright holder of this work and the author uses the Dutch legislation to make this work public.

Applied Physics Letters

Lightly strained germanium quantum wells with hole mobility exceeding one million

Cite as: Appl. Phys. Lett. **120**, 122104 (2022); https://doi.org/10.1063/5.0083161
Submitted: 22 December 2021 • Accepted: 05 February 2022 • Published Online: 21 March 2022

M. Lodari, O. Kong, M. Rendell, et al.

COLLECTIONS

This paper was selected as Featured

View Online

Export Citation

CrossMark

ARTICLES YOU MAY BE INTERESTED IN

Design methodologies and fabrication of 4H-SiC lateral Schottky barrier diode on thin RESURF layer
Applied Physics Letters **120**, 122103 (2022); https://doi.org/10.1063/5.0081106

Thermo-mechanical aspects of gamma irradiation effects on GaN HEMTs
Applied Physics Letters **120**, 124101 (2022); https://doi.org/10.1063/5.0087209

Cubic boron nitride as a material for future electron device applications: A comparative analysis
Applied Physics Letters **120**, 122105 (2022); https://doi.org/10.1063/5.0084360

Lock-in Amplifiers up to 600 MHz

© 2022 Author(s).

Applied Physics Letters ARTICLE scitation.org/journal/apl

Lightly strained germanium quantum wells with hole mobility exceeding one million

Cite as: Appl. Phys. Lett. **120**, 122104 (2022); doi: 10.1063/5.0083161
Submitted: 22 December 2021 · Accepted: 5 February 2022 ·
Published Online: 21 March 2022

View Online

Export Citation
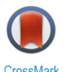
CrossMark

M. Lodari,[1] O. Kong,[2,3] M. Rendell,[2,3] A. Tosato,[1] A. Sammak,[4] M. Veldhorst,[1] A. R. Hamilton,[2,3] and G. Scappucci[1,a)]

AFFILIATIONS

[1]QuTech and Kavli Institute of Nanoscience, Delft University of Technology, PO Box 5046, 2600 GA Delft, The Netherlands
[2]School of Physics, University of New South Wales, Sydney, New South Wales 2052, Australia
[3]ARC Centre of Excellence for Future Low-Energy Electronics Technologies, University of New South Wales, Sydney, New South Wales 2052, Australia
[4]QuTech and Netherlands Organisation for Applied Scientific Research (TNO), Delft, The Netherlands

[a)]**Author to whom correspondence should be addressed:** g.scappucci@tudelft.nl

ABSTRACT

We demonstrate that a lightly strained germanium channel ($\varepsilon_{//} = -0.41\%$) in an undoped Ge/$Si_{0.1}Ge_{0.9}$ heterostructure field effect transistor supports a two-dimensional (2D) hole gas with mobility in excess of 1×10^6 cm^2/Vs and percolation density less than 5×10^{10} cm^{-2}. This low disorder 2D hole system shows tunable fractional quantum Hall effects at low densities and low magnetic fields. The low-disorder and small effective mass ($0.068m_e$) defines lightly strained germanium as a basis to tune the strength of the spin–orbit coupling for fast and coherent quantum hardware.

Published under an exclusive license by AIP Publishing. https://doi.org/10.1063/5.0083161

Quantum confined holes in germanium are emerging as a compelling platform for quantum information processing because of several favorable properties.[1] The light hole effective mass ($\sim 0.05m_e$ at zero density)[2] and the absence of valley degeneracy[3,4] give rise to large orbital splittings in quantum dots.[5] The intrinsic sizable and tunable spin–orbit coupling (SOC)[6,7] enables all-electrical fast qubit driving.[8–11] Furthermore, the capability to host superconducting pairing correlations[12–14] is promising for co-integration of spin-qubits with superconductors in hybrid architectures for spin–spin long-distance entanglement and quantum information transfer between different qubit types.[15–21]

Planar Ge/SiGe heterostructures are promising for scaling up to large quantum processors due to their compatibility with advanced semiconductor manufacturing.[22] The low-disorder in planar Ge quantum wells[23] (QWs) enabled the demonstration of a four-qubit quantum processor based on hole spins in a two-by-two array of quantum dots.[24] These heterostructures featured a $Si_{0.2}Ge_{0.8}$ strain-relaxed buffer (SRB), resulting in quantum wells with compressive strain $\varepsilon_{//} = -0.63\%$.[25] Alternatively, higher strained Ge ($\varepsilon_{//} = -1.18\,\%$) on $Si_{0.25}Ge_{0.75}$ SRBs enabled singlet–triplet spin qubits.[26] Lightly strained Ge/SiGe heterostructures are unexplored and could offer potentially larger SOC because of the reduced energy splitting between heavy holes (HHs) and light holes (LHs),[27] which is ≈17 meV for Ge/$Si_{0.1}Ge_{0.9}$ compared to ≈51 meV for Ge/$Si_{0.2}Ge_{0.8}$, respectively.[3,4] As such, lightly strained Ge is interesting for exploring faster spin-qubit driving and for topological devices. In this Letter, we demonstrate that lightly strained Ge quantum wells in undoped Ge/$Si_{0.1}Ge_{0.9}$ support a two-dimensional hole gas (2DHG) with low disorder at low densities, a prerequisite for further exploration of lightly strained Ge quantum devices.

We grow the Ge/SiGe heterostructure by reduced-pressure chemical vapor deposition on a Si(001) wafer, and then we fabricate Hall-bar shaped heterostructure field effect transistors (H-FETs) with the same process as in Refs. 2, 23, and 25. Here, a 16 nm strained Ge (sGe) quantum well (QW) is positioned between two strain-relaxed layers of $Si_{0.1}Ge_{0.9}$ at a depth of 66 nm [schematics in Fig. 1(a)].[28] Applying a negative DC bias to the accumulation gate V_g induces a 2DHG at the Ge/$Si_{0.1}Ge_{0.9}$ interface. The density in the 2DHG p is increased above the percolation density p_p by making V_g more negative. We use standard four-probe low-frequency lock-in techniques for mobility-density and magnetotransport characterization at $T = 1.7$ K and 70 mK with the excitation source-drain bias of 1 mV and 100 μeV, respectively. We do not measure gate to drain current leakage over the range of applied V_g. Figure 1(b) shows the Raman spectra measured

Published under an exclusive license by AIP Publishing

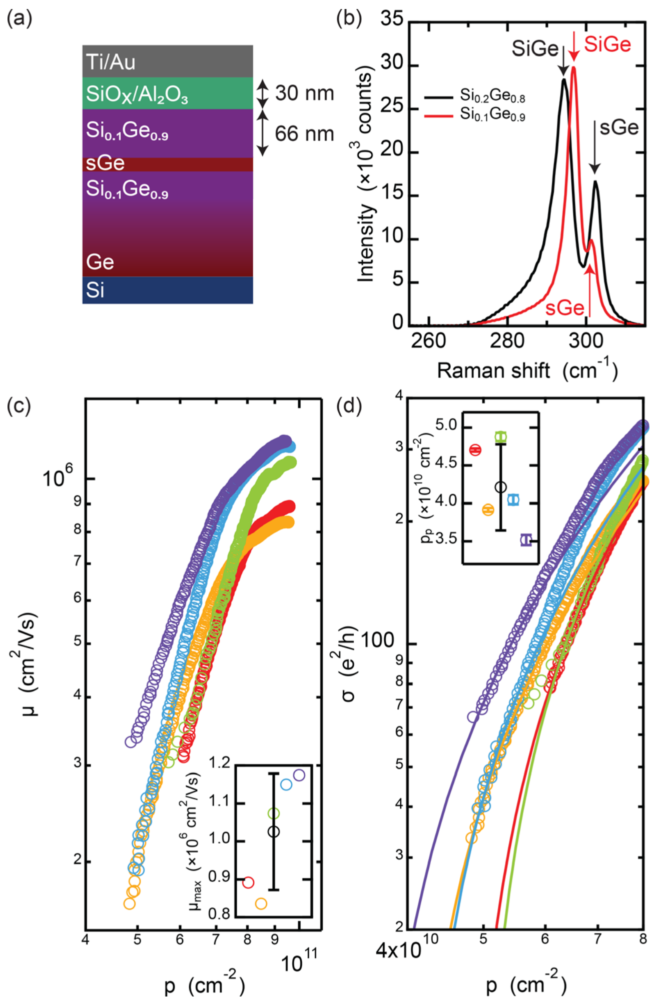

FIG. 1. (a) Schematic of a Ge/SiGe heterostructure field effect transistor. The strained Ge QW (sGe) is grown with the same lattice parameter to a $Si_{0.1}Ge_{0.9}$ SRB obtained by reverse grading, and it is separated from the native-SiO_x/Al_2O_3 dielectric and from the Ti/Au metallic gate stack by a 66 nm thick $Si_{0.1}Ge_{0.9}$ layer. (b) Intensity spectra as a function of the Raman shift from $Ge/Si_{0.2}Ge_{0.8}$ (black) and $Ge/Si_{0.1}Ge_{0.9}$ (red) heterostructures. (c) Mobility μ as a function of density p at $T = 1.7$ K from five Hall bar devices from the same wafer. The inset shows the maximum mobility μ_{max} from all the devices and average value $\pm$ standard deviation (black). (d) Conductivity σ_{xx} as a function of density p (circles) and fit to the percolation theory in the low density regime (solid lines). The inset shows the percolation density p_p from all the devices and average value $\pm$ standard deviation (black).

with a 633 nm red laser to determine the strain in the Ge QW. Comparing $Ge/Si_{0.1}Ge_{0.9}$ (red) to a control $Ge/Si_{0.2}Ge_{0.8}$ (black), we observe the Raman peak from the Ge–Ge vibration mode (sGe) in the QW appearing at a lower Raman shift. Conversely, the Raman peak from the SiGe layer is appearing at a higher Raman shift. These observations are consistent with the QW in $Ge/Si_{0.1}Ge_{0.9}$ being less strained due to a Ge-richer SiGe SRB.[29] From the position of the Raman shift (301.7 cm^{-1}), we estimate a light compressive strain of $\varepsilon_{//} = -0.41\%$ for the QW in $Ge/Si_{0.1}Ge_{0.9}$. This is significantly lower than in Refs. 25 and 26.

Moving on to electrical characterization, we operate the H-FET as follows. We turn on the device at $V_g \sim -0.4$ V and sweep V_g to larger negative voltages ($V_g \approx -9$ V) to saturate the traps at the semiconductor/dielectric interface via charge tunneling from the quantum well, similarly to what observed in shallow $Ge/Si_{0.2}Ge_{0.8}$ H-FETs.[25] At these large gate voltages, the density reaches saturation (p_{sat}) when the Fermi level crosses the surface quantum well at the $Si_{0.1}SiGe_{0.9}$/dielectric interface,[30] thereby screening the electric field at the sGe QW.[31] Figure 1(c) shows the mobility μ as a function of the Hall density p from five H-FETs fabricated on a 2×2 cm^2 coupon from the center of the 100 mm wafer and measured at $T = 1.7$ K. The mobility increases steeply with p due to the increasing screening of scattering from remote charged impurities.[31–33] At higher densities ($p \geq 7 \times 10^{10}$ cm^{-2}), short range scattering from impurities within and/or in proximity of the quantum well becomes the mobility-limiting scattering mechanism.[31] We observe a maximum mobility μ_{max} in the range of $0.8 - 1.2 \times 10^6$ cm^2/Vs for p_{sat} in the range of $9.43 - 9.64 \times 10^{10}$ cm^{-2} over the five investigated H-FETs. The inset in Fig. 1(c) shows a box plot of μ_{max} across the devices with an average value of $(1.03 \pm 0.15) \times 10^6$ cm^2/Vs (black), setting a benchmark for holes in buried channel transistors. Crucially, such high mobility is measured at very low densities below $p = 1 \times 10^{11}$ cm^{-2}, a significant improvement compared to previous studies in Ge/SiGe.[23,25]

Beyond μ_{max}, p_p is a key metric for characterizing the disorder potential landscape at low densities, the regime relevant for quantum dot qubits. Figure 1(d) shows the conductivity σ_{xx} (circles) as a function of density p for all investigated devices and their fit to the percolation theory (lines) $\sigma \sim (p - p_p)^{1.31}$, where the exponent 1.31 is fixed for 2D systems.[34] p_p ranges from 3.5 to 4.8×10^{10} cm^{-2}. The inset of Fig. 1(d) shows a box plot of the percolation density p_p across the devices with an average value of $p_p = (4.2 \pm 0.6) \times 10^{10}$ cm^{-2} (black). We take these values as an upper bound for p_p, since we observed smaller values of p_p [$(1.76 \pm 0.04) \times 10^{10}$ cm^{-2} at $T = 70$ mK] if the range of the applied gate voltage is restricted to small voltages above the turn-on threshold.

Since $Ge/S_{0.1}Ge_{0.9}$ is characterized by such a low level of disorder, we further explored the quantum transport proprieties of the 2DHG at 70 mK. Figure 2(a) shows the longitudinal resistivity ρ_{xx} (black) and transverse Hall resistivity ρ_{xy} (red) as a function of the perpendicular magnetic field B up to 0.75 T and at a Hall density of 7.2×10^{10} cm^{-2} and $\mu = 8.1 \times 10^5$ cm^2/Vs. We observe clear Shubnikov–de Haas (SdH) resistivity oscillations above 80 mT. The onset for resolving the spin-degeneracy by Zeeman splitting is 0.17 T, and ρ_{xx} minima reach zero already at 0.5 T. We do not observe beatings in the SdH oscillations associated with increased Rashba spin-splitting. We speculate that such beatings are more likely to be visible at higher densities that require the quantum well to be closer to the dielectric interface.[2]

Figure 3(b) shows the SdH oscillations at higher magnetic fields: strong minima are developed for filling factors ν with integer and fractional values. Clear plateaus are visible in ρ_{xy} for $\nu = 2/3$ and 1/3, where correspondingly ρ_{xx} vanishes. Such a high quality fractional quantum Hall effect (FQHE) has previously only been reported holes in modulation-doped systems at higher carrier densities and, hence, at larger magnetic fields.[35–37] Here, in the undoped heterostructure, we use the top-gate to follow the evolution of FQHE states down to low densities, providing avenues for studying the underlying physics.

Published under an exclusive license by AIP Publishing

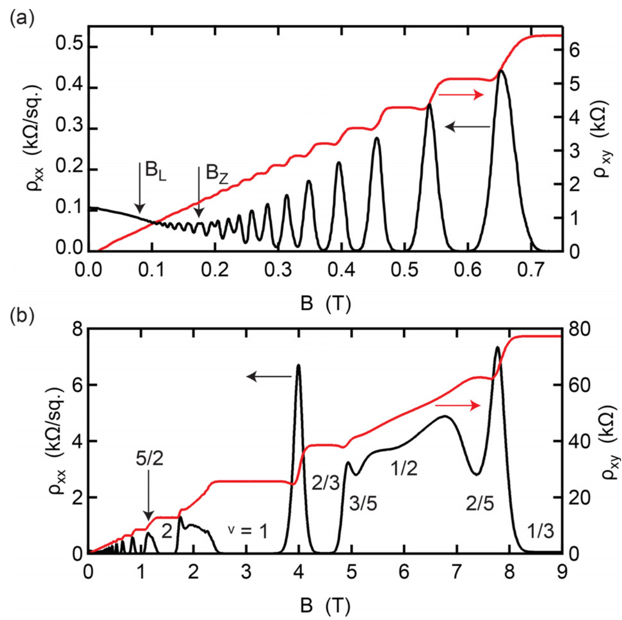

FIG. 2. Longitudinal resistivity ρ_{xx} (black) and transverse Hall resistivity ρ_{xy} (red) as a function of the perpendicular magnetic field B at 70 mK at a density of $p = 7.2 \times 10^{10}$ cm^{-2} and mobility $\mu = 8.1 \times 10^5$ cm^2/Vs. (a) Low-field Shubnikov–de Haas oscillations from $B = 0$ to 0.75 T and (b) in an expanded magnetic field range from $B = 0$ to 9 T. Onset of Landau levels (B_L) and Zeeman splitting (B_Z) are reported. Integer and fractional Landau level labels are reported.

The color map in Fig. 3(a), measured at $T = 70$ mK, shows ρ_{xx} (normalized to the value $\rho_{xx,0}$ at zero magnetic field) as a function of the magnetic field B and Hall density p in the range of 4.1–7.1 $\times 10^{10}$ cm^{-2}. Yellow and blue regions in the color map correspond to peaks and dips in the normalized ρ_{xx}, highlighting the density-dependent evolution of integer and fractional filling factors. All filling factors fan out toward the higher magnetic field and density, and fractional filling factors are well resolved across the full investigated range of the density and magnetic field. Three line cuts from the color map are shown in Figs. 3(b)–3(d) at decreasing density $p = 7.1$ (blue), 5.9 (green), and 4.2×10^{10} cm^{-2} (red), respectively. We observe that the minima associated with fractional ν become shallower as the density is decreased, possibly because of increased level broadening by unscreened disorder and because of weaker Coulomb interactions and correlation effects.[36,37] We also observe the distance between the onset of Shubnikov–de Haas oscillations (B_L) and Zeeman splitting (B_Z) reducing from Fig. 3(b) to Fig. 3(c). In Fig. 3(d), B_L and B_Z have crossed, meaning that at $p = 4.2 \times 10^{10}$ cm^{-2}, the Zeeman gap is larger than the cyclotron gap and, therefore, the spin susceptibility $(g^* m^*)/m_e \geq 1$,[38] where m^* is the effective mass and g^* is the effective g-factor out of plane. Indeed, from thermal activation measurement (the supplementary material), we estimate $m^* = (0.068 \pm 0.001) m_e$ and $g^* = 13.95 \pm 0.18$ at a density of 5.8×10^{10} cm^{-2}, corresponding to a spin susceptibility of ≈ 1. We note that similar values of m^* and g^* were reported in Ge/$Si_{0.2}Ge_{0.8}$ (Refs. 2 and 5) albeit at much higher density, pointing to higher HH–LH intermixing in the lightly strained quantum wells at lower densities, as expected from theory.[3]

In conclusion, we demonstrated a lightly strained Ge/SiGe heterostrucure supporting a 2DHG with mobility in excess of one million and low percolation densities (less than 5×10^{10} cm^{-2}). Such a low disorder enables measurement of FQHE at tunable low densities and low magnetic fields. To mitigate the effect of traps at the interface and to suppress tunneling from the quantum well to the surface, we speculate that lightly strained Ge channels could be positioned deeper compared to more strained channels[23,30] because of the smaller band offset ($\approx$66 meV Ge/$Si_{0.2}Ge_{0.9}$ vs $\approx$130 meV in Ge/$Si_{0.2}Ge_{0.8}$). Further measurements in quantum dots, where confinement increases the HH–LH

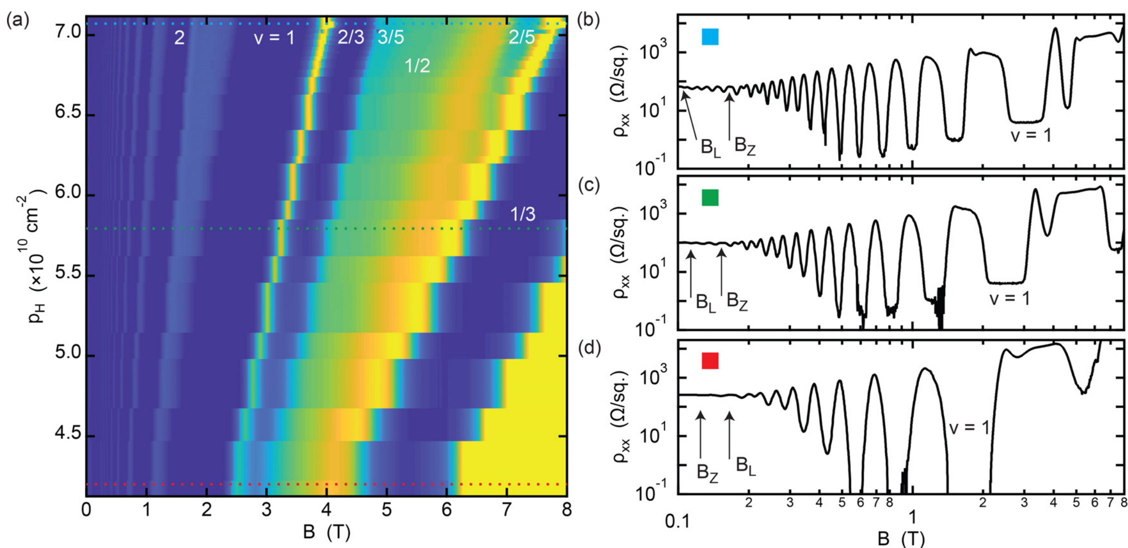

FIG. 3. (a) Normalized longitudinal resistivity $\rho_{xx}/\rho_{xx,0}$ as a function of the magnetic field B and Hall density p at $T = 70$ mK. Labels of integer and fractional ν assigned from the quantum Hall effect are reported. Amplitude color scale: 0 to 60. Dashed lines corresponding to the line cuts ρ_{xx} vs B at different densities are reported for (b) $p = 7.1$, (c) 5.9, and (d) 4.2×10^{10} cm^{-2}. Labels of Landau levels (B_L) and Zeeman splitting (B_Z) onset are reported.

Published under an exclusive license by AIP Publishing

mixing, will help us to elucidate the effect of reduced strain on the spin–orbit coupling in the system. The demonstration that holes can be defined in QWs with varying strain provides avenues to explore the opportunities in the germanium quantum information route.

See the supplementary material for measurements of the effective g-factor and effective mass.

G.S. and M.V. acknowledge support through a projectruimte grant associated with the Netherlands Organization of Scientific Research (NWO). This work was partially funded by the ARC Centre of Excellence for Future Low Energy Electronics Technologies (No. CE170100039).

AUTHOR DECLARATIONS

Conflict of Interest

The authors have no conflicts to disclose.

Author Contributions

M.L. and O.K. contributed equally to this work.

DATA AVAILABILITY

The data that support the findings of this study are openly available in 4TU Research Data at doi.org/10.4121/17306906.v1, Ref. 39.

REFERENCES

[1] G. Scappucci, C. Kloeffel, F. A. Zwanenburg, D. Loss, M. Myronov, J.-J. Zhang, S. De Franceschi, G. Katsaros, and M. Veldhorst, Nat. Rev. Mater. **6**, 926 (2021).
[2] M. Lodari, A. Tosato, D. Sabbagh, M. A. Schubert, G. Capellini, A. Sammak, M. Veldhorst, and G. Scappucci, Phys. Rev. B **100**, 041304 (2019).
[3] L. A. Terrazos, E. Marcellina, Z. Wang, S. N. Coppersmith, M. Friesen, A. R. Hamilton, X. Hu, B. Koiller, A. L. Saraiva, D. Culcer, and R. B. Capaz, Phys. Rev. B **103**, 125201 (2021).
[4] P. Del Vecchio, M. Lodari, A. Sammak, G. Scappucci, and O. Moutanabbir, Phys. Rev. B **102**, 115304 (2020).
[5] N. W. Hendrickx, D. P. Franke, A. Sammak, M. Kouwenhoven, D. Sabbagh, L. Yeoh, R. Li, M. L. Tagliaferri, M. Virgilio, G. Capellini, G. Scappucci, and M. Veldhorst, Nat. Commun. **9**, 2835 (2018).
[6] F. N. M. Froning, M. J. Rančić, B. Hetényi, S. Bosco, M. K. Rehmann, A. Li, E. P. A. M. Bakkers, F. A. Zwanenburg, D. Loss, D. M. Zumbühl, and F. R. Braakman, Phys. Rev. Res. **3**, 013081 (2021).
[7] S. Bosco, M. Benito, C. Adelsberger, and D. Loss, Phys. Rev. B **104**, 115425 (2021).
[8] H. Watzinger, J. Kukučka, L. Vukušić, F. Gao, T. Wang, F. Schäffler, J.-J. Zhang, and G. Katsaros, Nat. Commun. **9**, 3902 (2018).
[9] N. W. Hendrickx, D. P. Franke, A. Sammak, G. Scappucci, and M. Veldhorst, Nature **577**, 487 (2020).
[10] F. N. M. Froning, L. C. Camenzind, O. A. H. van der Molen, A. Li, E. P. A. M. Bakkers, D. M. Zumbühl, and F. R. Braakman, Nat. Nanotechnol. **16**, 308 (2021).
[11] K. Wang, G. Xu, F. Gao, H. Liu, R.-L. Ma, X. Zhang, Z. Wang, G. Cao, T. Wang, J.-J. Zhang, D. Culcer, X. Hu, H.-W. Jiang, H.-O. Li, G.-C. Guo, and G.-P. Guo, Nat. Commun. **13**, 206 (2022).
[12] R. Mizokuchi, R. Maurand, F. Vigneau, M. Myronov, and S. De Franceschi, Nano Lett. **18**, 4861 (2018).
[13] N. W. Hendrickx, M. L. V. Tagliaferri, M. Kouwenhoven, R. Li, D. P. Franke, A. Sammak, A. Brinkman, G. Scappucci, and M. Veldhorst, Phys. Rev. B **99**, 075435 (2019).
[14] K. Aggarwal, A. Hofmann, D. Jirovec, I. Prieto, A. Sammak, M. Botifoll, S. Martí-Sánchez, M. Veldhorst, J. Arbiol, G. Scappucci, J. Danon, and G. Katsaros, Phys. Rev. Res. **3**, L022005 (2021).
[15] M.-S. Choi, C. Bruder, and D. Loss, Phys. Rev. B **62**, 13569 (2000).
[16] X. Hu, Y.-x. Liu, and F. Nori, Phys. Rev. B **86**, 035314 (2012).
[17] M. Leijnse and K. Flensberg, Phys. Rev. B **86**, 104511 (2012).
[18] M. Leijnse and K. Flensberg, Phys. Rev. Lett. **111**, 060501 (2013).
[19] F. Hassler, G. Catelani, and H. Bluhm, Phys. Rev. B **92**, 235401 (2015).
[20] S. Hoffman, C. Schrade, J. Klinovaja, and D. Loss, Phys. Rev. B **94**, 045316 (2016).
[21] M. J. Rančić, S. Hoffman, C. Schrade, J. Klinovaja, and D. Loss, Phys. Rev. B **99**, 165306 (2019).
[22] R. Pillarisetty, Nature **479**, 324 (2011).
[23] M. Lodari, N. W. Hendrickx, W. I. L. Lawrie, T.-K. Hsiao, L. M. K. Vandersypen, A. Sammak, M. Veldhorst, and G. Scappucci, Mater. Quantum Technol. **1**, 011002 (2021).
[24] N. W. Hendrickx, W. I. L. Lawrie, M. Russ, F. van Riggelen, S. L. de Snoo, R. N. Schouten, A. Sammak, G. Scappucci, and M. Veldhorst, Nature **591**, 580 (2021).
[25] A. Sammak, D. Sabbagh, N. W. Hendrickx, M. Lodari, B. Paquelet Wuetz, A. Tosato, L. R. Yeoh, M. Bollani, M. Virgilio, M. A. Schubert, P. Zaumseil, G. Capellini, M. Veldhorst, and G. Scappucci, Adv. Funct. Mater. **29**, 1807613 (2019).
[26] D. Jirovec, A. Hofmann, A. Ballabio, P. M. Mutter, G. Tavani, M. Botifoll, A. Crippa, J. Kukucka, O. Sagi, F. Martins, J. Saez-Mollejo, I. Prieto, M. Borovkov, J. Arbiol, D. Chrastina, G. Isella, and G. Katsaros, Nat. Mater. **20**, 1106 (2021).
[27] R. Moriya, K. Sawano, Y. Hoshi, S. Masubuchi, Y. Shiraki, A. Wild, C. Neumann, G. Abstreiter, D. Bougeard, T. Koga, and T. Machida, Phys. Rev. Lett. **113**, 086601 (2014).
[28] The chemical composition of the layers is measured by secondary ion mass spectroscopy.
[29] F. Pezzoli, E. Bonera, E. Grilli, M. Guzzi, S. Sanguinetti, D. Chrastina, G. Isella, H. von Känel, E. Wintersberger, J. Stangl, and G. Bauer, J. Appl. Phys. **103**, 093521 (2008).
[30] Y.-H. Su, Y. Chuang, C.-Y. Liu, J.-Y. Li, and T.-M. Lu, Phys. Rev. Mater. **1**, 044601 (2017).
[31] D. Laroche, S. H. Huang, Y. Chuang, J. Y. Li, C. W. Liu, and T. M. Lu, Appl. Phys. Lett. **108**, 233504 (2016).
[32] D. Monroe, J. Vacuum Sci. Technol., B **11**, 1731 (1993).
[33] A. Gold, J. Appl. Phys. **108**, 063710 (2010).
[34] L. A. Tracy, E. H. Hwang, K. Eng, G. A. Ten Eyck, E. P. Nordberg, K. Childs, M. S. Carroll, M. P. Lilly, and S. Das Sarma, Phys. Rev. B **79**, 235307 (2009).
[35] Q. Shi, M. A. Zudov, C. Morrison, and M. Myronov, Phys. Rev. B **91**, 241303 (2015).
[36] O. A. Mironov, N. d'Ambrumenil, A. Dobbie, D. R. Leadley, A. V. Suslov, and E. Green, Phys. Rev. Lett. **116**, 176802 (2016).
[37] I. B. Berkutov, V. V. Andrievskii, Y. A. Kolesnichenko, and O. A. Mironov, Low Temp. Phys. **45**, 1202 (2019).
[38] T. M. Lu, L. A. Tracy, D. Laroche, S.-H. Huang, Y. Chuang, Y.-H. Su, J.-Y. Li, and C. W. Liu, Sci. Rep. **7**, 2468 (2017).
[39] M. Lodari, G. Scappucci, A. R. Hamilton, O. Kong, and M. Rendell (2021). "Lightly-strained germanium quantum wells with hole mobility exceeding one million," 4TU.ResearchData. Dataset. https://doi.org/10.4121/17306906.v1

Published under an exclusive license by AIP Publishing

Applied Physics Letters

RESEARCH ARTICLE | MARCH 21 2022

Lightly strained germanium quantum wells with hole mobility exceeding one million

M. Lodari; O. Kong; M. Rendell; A. Tosato; A. Sammak; M. Veldhorst; A. R. Hamilton; G. Scappucci

Appl. Phys. Lett. 120, 122104 (2022)
https://doi.org/10.1063/5.0083161

CrossMark

20 February 2024 09:31:28

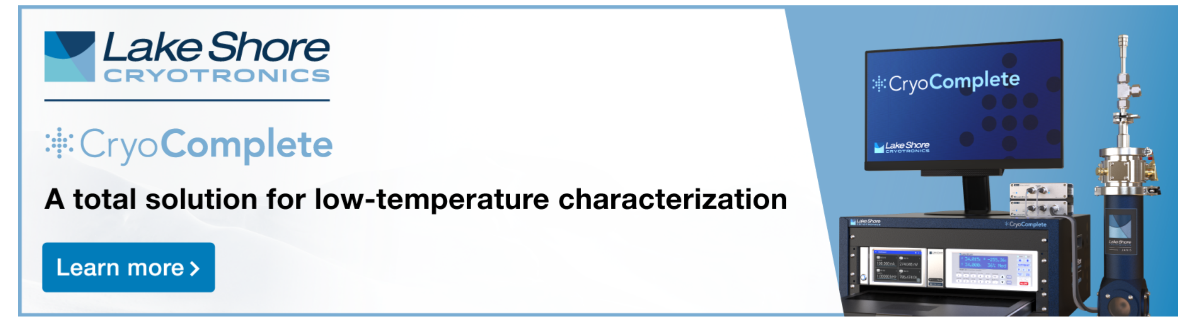

Applied Physics Letters ARTICLE scitation.org/journal/apl

Lightly strained germanium quantum wells with hole mobility exceeding one million

Cite as: Appl. Phys. Lett. **120**, 122104 (2022); doi: 10.1063/5.0083161
Submitted: 22 December 2021 · Accepted: 5 February 2022 ·
Published Online: 21 March 2022

View Online

Export Citation

CrossMark

M. Lodari,[1] O. Kong,[2,3] M. Rendell,[2,3] A. Tosato,[1] A. Sammak,[4] M. Veldhorst,[1] A. R. Hamilton,[2,3] and G. Scappucci[1,a)]

AFFILIATIONS

[1]QuTech and Kavli Institute of Nanoscience, Delft University of Technology, PO Box 5046, 2600 GA Delft, The Netherlands
[2]School of Physics, University of New South Wales, Sydney, New South Wales 2052, Australia
[3]ARC Centre of Excellence for Future Low-Energy Electronics Technologies, University of New South Wales, Sydney, New South Wales 2052, Australia
[4]QuTech and Netherlands Organisation for Applied Scientific Research (TNO), Delft, The Netherlands

[a)]Author to whom correspondence should be addressed: g.scappucci@tudelft.nl

ABSTRACT

We demonstrate that a lightly strained germanium channel ($\varepsilon_{//} = -0.41\%$) in an undoped Ge/$Si_{0.1}Ge_{0.9}$ heterostructure field effect transistor supports a two-dimensional (2D) hole gas with mobility in excess of 1×10^6 cm^2/Vs and percolation density less than 5×10^{10} cm^{-2}. This low disorder 2D hole system shows tunable fractional quantum Hall effects at low densities and low magnetic fields. The low-disorder and small effective mass ($0.068m_e$) defines lightly strained germanium as a basis to tune the strength of the spin–orbit coupling for fast and coherent quantum hardware.

Published under an exclusive license by AIP Publishing. https://doi.org/10.1063/5.0083161

20 February 2024 09:31:28

Quantum confined holes in germanium are emerging as a compelling platform for quantum information processing because of several favorable properties.[1] The light hole effective mass ($\sim 0.05m_e$ at zero density)[2] and the absence of valley degeneracy[3,4] give rise to large orbital splittings in quantum dots.[5] The intrinsic sizable and tunable spin–orbit coupling (SOC)[6,7] enables all-electrical fast qubit driving.[8–11] Furthermore, the capability to host superconducting pairing correlations[12–14] is promising for co-integration of spin-qubits with superconductors in hybrid architectures for spin–spin long-distance entanglement and quantum information transfer between different qubit types.[15–21]

Planar Ge/SiGe heterostructures are promising for scaling up to large quantum processors due to their compatibility with advanced semiconductor manufacturing.[22] The low-disorder in planar Ge quantum wells[23] (QWs) enabled the demonstration of a four-qubit quantum processor based on hole spins in a two-by-two array of quantum dots.[24] These heterostructures featured a $Si_{0.2}Ge_{0.8}$ strain-relaxed buffer (SRB), resulting in quantum wells with compressive strain $\varepsilon_{//} = -0.63\%$.[25] Alternatively, higher strained Ge ($\varepsilon_{//} = -1.18\,\%$) on $Si_{0.25}Ge_{0.75}$ SRBs enabled singlet–triplet spin qubits.[26] Lightly strained Ge/SiGe heterostructures are unexplored and could offer potentially larger SOC because of the reduced energy splitting between heavy holes (HHs) and light holes (LHs),[27] which is $\approx$17 meV for Ge/$Si_{0.1}Ge_{0.9}$ compared to $\approx$51 meV for Ge/$Si_{0.2}Ge_{0.8}$, respectively.[3,4] As such, lightly strained Ge is interesting for exploring faster spin-qubit driving and for topological devices. In this Letter, we demonstrate that lightly strained Ge quantum wells in undoped Ge/$Si_{0.1}Ge_{0.9}$ support a two-dimensional hole gas (2DHG) with low disorder at low densities, a prerequisite for further exploration of lightly strained Ge quantum devices.

We grow the Ge/SiGe heterostructure by reduced-pressure chemical vapor deposition on a Si(001) wafer, and then we fabricate Hall-bar shaped heterostructure field effect transistors (H-FETs) with the same process as in Refs. 2, 23, and 25. Here, a 16 nm strained Ge (sGe) quantum well (QW) is positioned between two strain-relaxed layers of $Si_{0.1}Ge_{0.9}$ at a depth of 66 nm [schematics in Fig. 1(a)].[28] Applying a negative DC bias to the accumulation gate V_g induces a 2DHG at the Ge/$Si_{0.1}Ge_{0.9}$ interface. The density in the 2DHG p is increased above the percolation density p_p by making V_g more negative. We use standard four-probe low-frequency lock-in techniques for mobility-density and magnetotransport characterization at $T = 1.7$ K and 70 mK with the excitation source-drain bias of 1 mV and 100 μeV, respectively. We do not measure gate to drain current leakage over the range of applied V_g. Figure 1(b) shows the Raman spectra measured

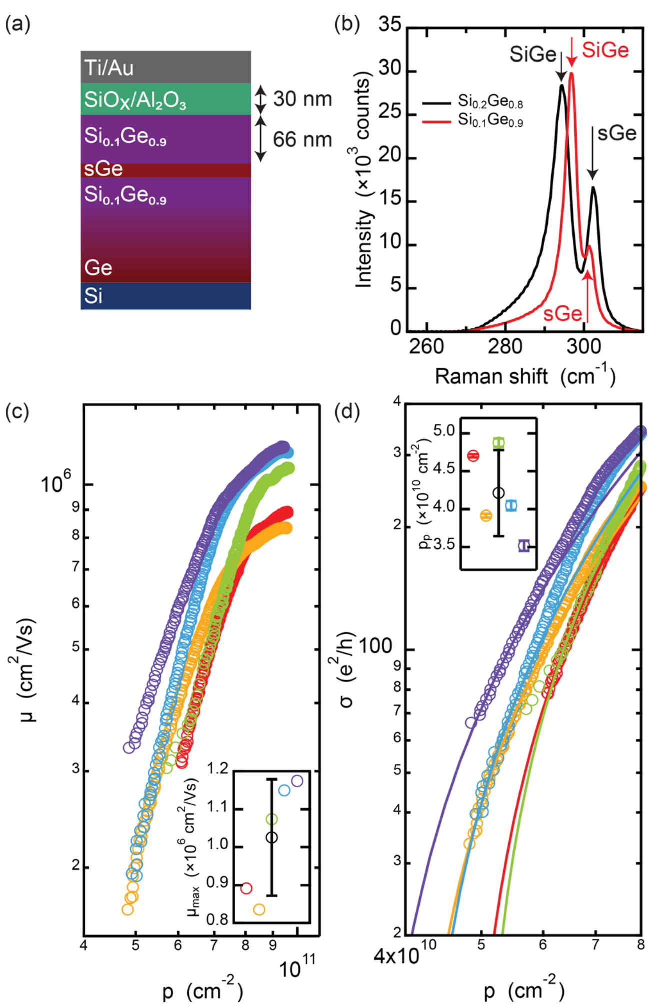

FIG. 1. (a) Schematic of a Ge/SiGe heterostructure field effect transistor. The strained Ge QW (sGe) is grown with the same lattice parameter to a $Si_{0.1}Ge_{0.9}$ SRB obtained by reverse grading, and it is separated from the native-SiO_x/Al_2O_3 dielectric and from the Ti/Au metallic gate stack by a 66 nm thick $Si_{0.1}Ge_{0.9}$ layer. (b) Intensity spectra as a function of the Raman shift from Ge/$Si_{0.2}Ge_{0.8}$ (black) and Ge/$Si_{0.1}Ge_{0.9}$ (red) heterostructures. (c) Mobility μ as a function of density p at $T = 1.7$ K from five Hall bar devices from the same wafer. The inset shows the maximum mobility μ_{max} from all the devices and average value ± standard deviation (black). (d) Conductivity σ_{xx} as a function of density p (circles) and fit to the percolation theory in the low density regime (solid lines). The inset shows the percolation density p_p from all the devices and average value ± standard deviation (black).

with a 633 nm red laser to determine the strain in the Ge QW. Comparing Ge/$Si_{0.1}Ge_{0.9}$ (red) to a control Ge/$Si_{0.2}Ge_{0.8}$ (black), we observe the Raman peak from the Ge–Ge vibration mode (sGe) in the QW appearing at a lower Raman shift. Conversely, the Raman peak from the SiGe layer is appearing at a higher Raman shift. These observations are consistent with the QW in Ge/$Si_{0.1}Ge_{0.9}$ being less strained due to a Ge-richer SiGe SRB.[29] From the position of the Raman shift (301.7 cm^{-1}), we estimate a light compressive strain of $\varepsilon_{//} = -0.41\%$ for the QW in Ge/$Si_{0.1}Ge_{0.9}$. This is significantly lower than in Refs. 25 and 26.

Moving on to electrical characterization, we operate the H-FET as follows. We turn on the device at $V_g \sim -0.4$ V and sweep V_g to larger negative voltages ($V_g \approx -9$ V) to saturate the traps at the semiconductor/dielectric interface via charge tunneling from the quantum well, similarly to what observed in shallow Ge/$Si_{0.2}Ge_{0.8}$ H-FETs.[25] At these large gate voltages, the density reaches saturation (p_{sat}) when the Fermi level crosses the surface quantum well at the $Si_{0.1}SiGe_{0.9}$/dielectric interface,[30] thereby screening the electric field at the sGe QW.[31] Figure 1(c) shows the mobility μ as a function of the Hall density p from five H-FETs fabricated on a $2 \times 2\,cm^2$ coupon from the center of the 100 mm wafer and measured at $T = 1.7$ K. The mobility increases steeply with p due to the increasing screening of scattering from remote charged impurities.[31–33] At higher densities ($p \geq 7 \times 10^{10}$ cm^{-2}), short range scattering from impurities within and/or in proximity of the quantum well becomes the mobility-limiting scattering mechanism.[31] We observe a maximum mobility μ_{max} in the range of $0.8 - 1.2 \times 10^6$ cm^2/Vs for p_{sat} in the range of $9.43 - 9.64 \times 10^{10}$ cm^{-2} over the five investigated H-FETs. The inset in Fig. 1(c) shows a box plot of μ_{max} across the devices with an average value of $(1.03 \pm 0.15) \times 10^6$ cm^2/Vs (black), setting a benchmark for holes in buried channel transistors. Crucially, such high mobility is measured at very low densities below $p = 1 \times 10^{11}$ cm^{-2}, a significant improvement compared to previous studies in Ge/SiGe.[23,25]

Beyond μ_{max}, p_p is a key metric for characterizing the disorder potential landscape at low densities, the regime relevant for quantum dot qubits. Figure 1(d) shows the conductivity σ_{xx} (circles) as a function of density p for all investigated devices and their fit to the percolation theory (lines) $\sigma \sim (p - p_p)^{1.31}$, where the exponent 1.31 is fixed for 2D systems.[34] p_p ranges from 3.5 to 4.8×10^{10} cm^{-2}. The inset of Fig. 1(d) shows a box plot of the percolation density p_p across the devices with an average value of $p_p = (4.2 \pm 0.6) \times 10^{10}$ cm^{-2} (black). We take these values as an upper bound for p_p, since we observed smaller values of p_p [$(1.76 \pm 0.04) \times 10^{10}$ cm^{-2} at $T = 70$ mK] if the range of the applied gate voltage is restricted to small voltages above the turn-on threshold.

Since Ge/$S_{0.1}Ge_{0.9}$ is characterized by such a low level of disorder, we further explored the quantum transport proprieties of the 2DHG at 70 mK. Figure 2(a) shows the longitudinal resistivity ρ_{xx} (black) and transverse Hall resistivity ρ_{xy} (red) as a function of the perpendicular magnetic field B up to 0.75 T and at a Hall density of 7.2×10^{10} cm^{-2} and $\mu = 8.1 \times 10^5$ cm^2/Vs. We observe clear Shubnikov–de Haas (SdH) resistivity oscillations above 80 mT. The onset for resolving the spin-degeneracy by Zeeman splitting is 0.17 T, and ρ_{xx} minima reach zero already at 0.5 T. We do not observe beatings in the SdH oscillations associated with increased Rashba spin-splitting. We speculate that such beatings are more likely to be visible at higher densities that require the quantum well to be closer to the dielectric interface.[2]

Figure 3(b) shows the SdH oscillations at higher magnetic fields: strong minima are developed for filling factors ν with integer and fractional values. Clear plateaus are visible in ρ_{xy} for $\nu = 2/3$ and 1/3, where correspondingly ρ_{xx} vanishes. Such a high quality fractional quantum Hall effect (FQHE) has previously only been reported holes in modulation-doped systems at higher carrier densities and, hence, at larger magnetic fields.[35–37] Here, in the undoped heterostructure, we use the top-gate to follow the evolution of FQHE states down to low densities, providing avenues for studying the underlying physics.

20 February 2024 09:31:28

Published under an exclusive license by AIP Publishing

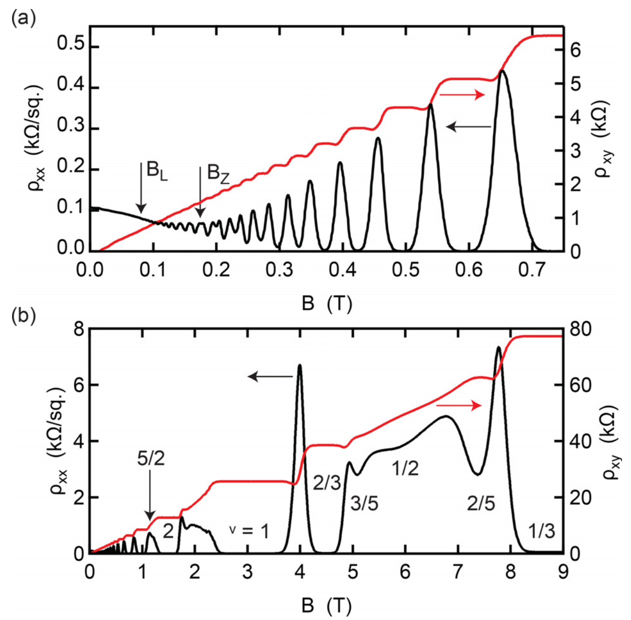

FIG. 2. Longitudinal resistivity ρ_{xx} (black) and transverse Hall resistivity ρ_{xy} (red) as a function of the perpendicular magnetic field B at 70 mK at a density of $p = 7.2 \times 10^{10}$ cm^{-2} and mobility $\mu = 8.1 \times 10^5$ cm^2/Vs. (a) Low-field Shubnikov–de Haas oscillations from $B = 0$ to 0.75 T and (b) in an expanded magnetic field range from $B = 0$ to 9 T. Onset of Landau levels (B_L) and Zeeman splitting (B_Z) are reported. Integer and fractional Landau level labels are reported.

The color map in Fig. 3(a), measured at $T = 70$ mK, shows ρ_{xx} (normalized to the value $\rho_{xx,0}$ at zero magnetic field) as a function of the magnetic field B and Hall density p in the range of 4.1–7.1 $\times 10^{10}$ cm^{-2}. Yellow and blue regions in the color map correspond to peaks and dips in the normalized ρ_{xx}, highlighting the density-dependent evolution of integer and fractional filling factors. All filling factors fan out toward the higher magnetic field and density, and fractional filling factors are well resolved across the full investigated range of the density and magnetic field. Three line cuts from the color map are shown in Figs. 3(b)–3(d) at decreasing density $p = 7.1$ (blue), 5.9 (green), and 4.2×10^{10} cm^{-2} (red), respectively. We observe that the minima associated with fractional ν become shallower as the density is decreased, possibly because of increased level broadening by unscreened disorder and because of weaker Coulomb interactions and correlation effects.[36,37] We also observe the distance between the onset of Shubnikov–de Haas oscillations (B_L) and Zeeman splitting (B_Z) reducing from Fig. 3(b) to Fig. 3(c). In Fig. 3(d), B_L and B_Z have crossed, meaning that at $p = 4.2 \times 10^{10}$ cm^{-2}, the Zeeman gap is larger than the cyclotron gap and, therefore, the spin susceptibility $(g^* m^*)/m_e \geq 1$,[38] where m^* is the effective mass and g^* is the effective g-factor out of plane. Indeed, from thermal activation measurement (the supplementary material), we estimate $m^* = (0.068 \pm 0.001)m_e$ and $g^* = 13.95 \pm 0.18$ at a density of 5.8×10^{10} cm^{-2}, corresponding to a spin susceptibility of ≈ 1. We note that similar values of m^* and g^* were reported in Ge/$Si_{0.2}Ge_{0.8}$ (Refs. 2 and 5) albeit at much higher density, pointing to higher HH–LH intermixing in the lightly strained quantum wells at lower densities, as expected from theory.[3]

In conclusion, we demonstrated a lightly strained Ge/SiGe heterostrucure supporting a 2DHG with mobility in excess of one million and low percolation densities (less than 5×10^{10} cm^{-2}). Such a low disorder enables measurement of FQHE at tunable low densities and low magnetic fields. To mitigate the effect of traps at the interface and to suppress tunneling from the quantum well to the surface, we speculate that lightly strained Ge channels could be positioned deeper compared to more strained channels[23,30] because of the smaller band offset ($\approx$66 meV Ge/$Si_{0.2}Ge_{0.9}$ vs $\approx$130 meV in Ge/$Si_{0.2}Ge_{0.8}$). Further measurements in quantum dots, where confinement increases the HH–LH

20 February 2024 09:31:28

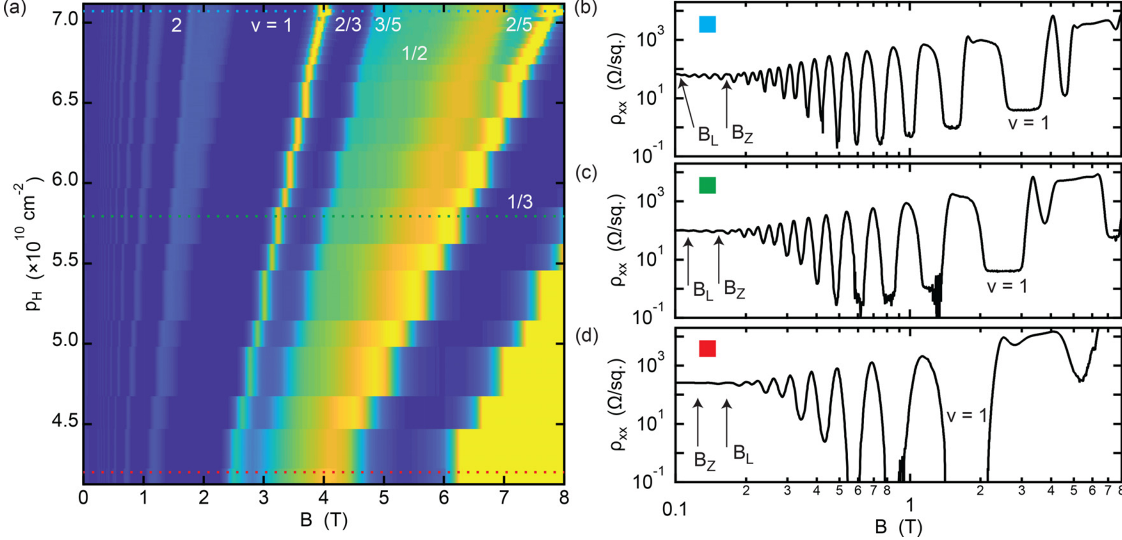

FIG. 3. (a) Normalized longitudinal resistivity $\rho_{xx}/\rho_{xx,0}$ as a function of the magnetic field B and Hall density p at $T = 70$ mK. Labels of integer and fractional ν assigned from the quantum Hall effect are reported. Amplitude color scale: 0 to 60. Dashed lines corresponding to the line cuts ρ_{xx} vs B at different densities are reported for (b) $p = 7.1$, (c) 5.9, and (d) 4.2×10^{10} cm^{-2}. Labels of Landau levels (B_L) and Zeeman splitting (B_Z) onset are reported.

Published under an exclusive license by AIP Publishing

mixing, will help us to elucidate the effect of reduced strain on the spin–orbit coupling in the system. The demonstration that holes can be defined in QWs with varying strain provides avenues to explore the opportunities in the germanium quantum information route.

See the supplementary material for measurements of the effective g-factor and effective mass.

G.S. and M.V. acknowledge support through a projectruimte grant associated with the Netherlands Organization of Scientific Research (NWO). This work was partially funded by the ARC Centre of Excellence for Future Low Energy Electronics Technologies (No. CE170100039).

AUTHOR DECLARATIONS

Conflict of Interest

The authors have no conflicts to disclose.

Author Contributions

M.L. and O.K. contributed equally to this work.

DATA AVAILABILITY

The data that support the findings of this study are openly available in 4TU Research Data at doi.org/10.4121/17306906.v1, Ref. 39.

REFERENCES

[1] G. Scappucci, C. Kloeffel, F. A. Zwanenburg, D. Loss, M. Myronov, J.-J. Zhang, S. De Franceschi, G. Katsaros, and M. Veldhorst, Nat. Rev. Mater. **6**, 926 (2021).
[2] M. Lodari, A. Tosato, D. Sabbagh, M. A. Schubert, G. Capellini, A. Sammak, M. Veldhorst, and G. Scappucci, Phys. Rev. B **100**, 041304 (2019).
[3] L. A. Terrazos, E. Marcellina, Z. Wang, S. N. Coppersmith, M. Friesen, A. R. Hamilton, X. Hu, B. Koiller, A. L. Saraiva, D. Culcer, and R. B. Capaz, Phys. Rev. B **103**, 125201 (2021).
[4] P. Del Vecchio, M. Lodari, A. Sammak, G. Scappucci, and O. Moutanabbir, Phys. Rev. B **102**, 115304 (2020).
[5] N. W. Hendrickx, D. P. Franke, A. Sammak, M. Kouwenhoven, D. Sabbagh, L. Yeoh, R. Li, M. L. Tagliaferri, M. Virgilio, G. Capellini, G. Scappucci, and M. Veldhorst, Nat. Commun. **9**, 2835 (2018).
[6] F. N. M. Froning, M. J. Rančić, B. Hetényi, S. Bosco, M. K. Rehmann, A. Li, E. P. A. M. Bakkers, F. A. Zwanenburg, D. Loss, D. M. Zumbühl, and F. R. Braakman, Phys. Rev. Res. **3**, 013081 (2021).
[7] S. Bosco, M. Benito, C. Adelsberger, and D. Loss, Phys. Rev. B **104**, 115425 (2021).
[8] H. Watzinger, J. Kukučka, L. Vukušić, F. Gao, T. Wang, F. Schäffler, J.-J. Zhang, and G. Katsaros, Nat. Commun. **9**, 3902 (2018).
[9] N. W. Hendrickx, D. P. Franke, A. Sammak, G. Scappucci, and M. Veldhorst, Nature **577**, 487 (2020).
[10] F. N. M. Froning, L. C. Camenzind, O. A. H. van der Molen, A. Li, E. P. A. M. Bakkers, D. M. Zumbühl, and F. R. Braakman, Nat. Nanotechnol. **16**, 308 (2021).
[11] K. Wang, G. Xu, F. Gao, H. Liu, R.-L. Ma, X. Zhang, Z. Wang, G. Cao, T. Wang, J.-J. Zhang, D. Culcer, X. Hu, H.-W. Jiang, H.-O. Li, G.-C. Guo, and G.-P. Guo, Nat. Commun. **13**, 206 (2022).
[12] R. Mizokuchi, R. Maurand, F. Vigneau, M. Myronov, and S. De Franceschi, Nano Lett. **18**, 4861 (2018).
[13] N. W. Hendrickx, M. L. V. Tagliaferri, M. Kouwenhoven, R. Li, D. P. Franke, A. Sammak, A. Brinkman, G. Scappucci, and M. Veldhorst, Phys. Rev. B **99**, 075435 (2019).
[14] K. Aggarwal, A. Hofmann, D. Jirovec, I. Prieto, A. Sammak, M. Botifoll, S. Martí-Sánchez, M. Veldhorst, J. Arbiol, G. Scappucci, J. Danon, and G. Katsaros, Phys. Rev. Res. **3**, L022005 (2021).
[15] M.-S. Choi, C. Bruder, and D. Loss, Phys. Rev. B **62**, 13569 (2000).
[16] X. Hu, Y.-x. Liu, and F. Nori, Phys. Rev. B **86**, 035314 (2012).
[17] M. Leijnse and K. Flensberg, Phys. Rev. B **86**, 104511 (2012).
[18] M. Leijnse and K. Flensberg, Phys. Rev. Lett. **111**, 060501 (2013).
[19] F. Hassler, G. Catelani, and H. Bluhm, Phys. Rev. B **92**, 235401 (2015).
[20] S. Hoffman, C. Schrade, J. Klinovaja, and D. Loss, Phys. Rev. B **94**, 045316 (2016).
[21] M. J. Rančić, S. Hoffman, C. Schrade, J. Klinovaja, and D. Loss, Phys. Rev. B **99**, 165306 (2019).
[22] R. Pillarisetty, Nature **479**, 324 (2011).
[23] M. Lodari, N. W. Hendrickx, W. I. L. Lawrie, T.-K. Hsiao, L. M. K. Vandersypen, A. Sammak, M. Veldhorst, and G. Scappucci, Mater. Quantum Technol. **1**, 011002 (2021).
[24] N. W. Hendrickx, W. I. L. Lawrie, M. Russ, F. van Riggelen, S. L. de Snoo, R. N. Schouten, A. Sammak, G. Scappucci, and M. Veldhorst, Nature **591**, 580 (2021).
[25] A. Sammak, D. Sabbagh, N. W. Hendrickx, M. Lodari, B. Paquelet Wuetz, A. Tosato, L. R. Yeoh, M. Bollani, M. Virgilio, M. A. Schubert, P. Zaumseil, G. Capellini, M. Veldhorst, and G. Scappucci, Adv. Funct. Mater. **29**, 1807613 (2019).
[26] D. Jirovec, A. Hofmann, A. Ballabio, P. M. Mutter, G. Tavani, M. Botifoll, A. Crippa, J. Kukucka, O. Sagi, F. Martins, J. Saez-Mollejo, I. Prieto, M. Borovkov, J. Arbiol, D. Chrastina, G. Isella, and G. Katsaros, Nat. Mater. **20**, 1106 (2021).
[27] R. Moriya, K. Sawano, Y. Hoshi, S. Masubuchi, Y. Shiraki, A. Wild, C. Neumann, G. Abstreiter, D. Bougeard, T. Koga, and T. Machida, Phys. Rev. Lett. **113**, 086601 (2014).
[28] The chemical composition of the layers is measured by secondary ion mass spectroscopy.
[29] F. Pezzoli, E. Bonera, E. Grilli, M. Guzzi, S. Sanguinetti, D. Chrastina, G. Isella, H. von Känel, E. Wintersberger, J. Stangl, and G. Bauer, J. Appl. Phys. **103**, 093521 (2008).
[30] Y.-H. Su, Y. Chuang, C.-Y. Liu, J.-Y. Li, and T.-M. Lu, Phys. Rev. Mater. **1**, 044601 (2017).
[31] D. Laroche, S. H. Huang, Y. Chuang, J. Y. Li, C. W. Liu, and T. M. Lu, Appl. Phys. Lett. **108**, 233504 (2016).
[32] D. Monroe, J. Vacuum Sci. Technol., B **11**, 1731 (1993).
[33] A. Gold, J. Appl. Phys. **108**, 063710 (2010).
[34] L. A. Tracy, E. H. Hwang, K. Eng, G. A. Ten Eyck, E. P. Nordberg, K. Childs, M. S. Carroll, M. P. Lilly, and S. Das Sarma, Phys. Rev. B **79**, 235307 (2009).
[35] Q. Shi, M. A. Zudov, C. Morrison, and M. Myronov, Phys. Rev. B **91**, 241303 (2015).
[36] O. A. Mironov, N. d'Ambrumenil, A. Dobbie, D. R. Leadley, A. V. Suslov, and E. Green, Phys. Rev. Lett. **116**, 176802 (2016).
[37] I. B. Berkutov, V. V. Andrievskii, Y. A. Kolesnichenko, and O. A. Mironov, Low Temp. Phys. **45**, 1202 (2019).
[38] T. M. Lu, L. A. Tracy, D. Laroche, S.-H. Huang, Y. Chuang, Y.-H. Su, J.-Y. Li, and C. W. Liu, Sci. Rep. **7**, 2468 (2017).
[39] M. Lodari, G. Scappucci, A. R. Hamilton, O. Kong, and M. Rendell (2021). "Lightly-strained germanium quantum wells with hole mobility exceeding one million," 4TU.ResearchData. Dataset. https://doi.org/10.4121/17306906.v1

20 February 2024 09:31:28

Published under an exclusive license by AIP Publishing